**RAA 2018** Vol. **18** No. **7**, 84(12pp) doi: 10.1088/1674–4527/18/7/84

*http://www.raa-journal.org* *http://iopscience.iop.org/raa*

*Research in Astronomy and Astrophysics*

# A particle-linkage model for non-axisymmetric elongated asteroids

Hong-Wei Yang[1,2], Shuang Li[1,2] and Cong Xu[3]

[1] College of Astronautics, Nanjing University of Aeronautics and Astronautics, Nanjing 210016, China; *lishuang@nuaa.edu.cn*

[2] Advanced Space Technology Laboratory, Nanjing University of Aeronautics and Astronautics, Nanjing 210016, China

[3] College of Mechanical and Electrical Engineering, Nanjing University of Aeronautics and Astronautics, Nanjing 210016, China

Received 2018 April 1; accepted 2018 April 12

**Abstract** This paper investigates a simplified model for describing the gravitational fields of non-axisymmetric elongated asteroids. The connection between the simplified model and the target asteroid is built by considering the positions of equilibrium points. To improve the performance of position matching for the equilibrium points associated with these non-axisymmetric asteroids, a non-axisymmetric triple-particle-linkage model is proposed based on two existing axisymmetric particle-linkage models. The unknown parameters of the simplified model are determined by minimizing the matching error using the nonlinear optimization method. The proposed simplified model is applied for three realistic elongated asteroids, 243 Ida, 433 Eros and (8567) 1996 HW1. The simulation results verify that the current particle-linkage model has better matching accuracy than the two existing particle-linkage models. The comparison, between the simplified model and the polyhedral model, on the topological cases of the equilibrium points and the distribution of gravitational potential further validate the rationality and accuracy of the simplified model.

**Key words:** asteroids: individual (243 Ida, 433 Eros, (8567) 1996 HW1) — celestial mechanics — gravitation

## 1 INTRODUCTION

In the past decade, several asteroid missions have been proposed or carried out by space agencies around the world. Among these missions, there are two asteroid sample return missions, *Hayabusa 2* and *OSIRIS-REx*, which are still ongoing. These missions demonstrate the importance of asteroid exploration and the associated great interest from space agencies.

Asteroid models are essential for studying the dynamics and designing orbits near asteroids. The polyhedral model (Werner & Scheeres 1996) is usually regarded as a precision model for irregularly shaped asteroids that does not have a problem with convergence (Scheeres et al. 2000). Thus, it has been widely used in studies of dynamics near asteroids such as equilibrium points (Yu & Baoyin 2012b; Jiang et al. 2014; Wang et al. 2014; Yang et al. 2018) and periodic orbits (Yu & Baoyin 2012a; Jiang 2015; Yu et al. 2015). However, this model usually has thousands of parameters (vertices and facets) that are needed to guarantee accuracy. Therefore, computation of the gravitational field by the polyhedral model can be time consuming. Moreover, it is hard to analyze the relationship between the dynamics and the model parameters. On the contrary, simplified models which approximate the gravitational field usually only have few parameters. Moreover, some simplified models have a simple analytical expression for computation of the gravitational field. Thus, it is convenient to analyze the effects of model parameters on the dynamics near asteroids such as the stability of equilibrium points (Zeng et al. 2015), the admissible hovering regions (Yang et al. 2015) and the distribution of stable periodic orbits (Lan et al. 2017). Besides, simplified models can also be used for helping designing orbits (Wang et al. 2017) and feedback control (Yang et al. 2017). Thus far, many simplified asteroid models have been proposed, such as the straight segment (Riaguas et al. 2001; Elipe & Lara 2003), double material segment (Bartczak & Breiter 2003), points and segments (Bartczak et al. 2006), the homogeneous cube (Liu et al. 2011), the dumbbell-shaped model (Li et al. 2013, 2017), the synchronous double ellipsoids model (Shang et al. 2015), the mass dipole model (Zeng et al. 2015), the triple-particle-linkage model (Lan et al. 2017) and the dipole segment model (Zeng et al. 2018).

Study on the connection between the simplified model and polyhedral model for natural elongated asteroids began in the work of Zeng et al. (2015). Their idea proposed determining parameters of the simplified model by matching the equilibrium points of the simplified model with those of the polyhedral model. The employed simplified model is the so-called mass dipole model where the two primaries are connected by a massless rigid rod. This model is also referred to as the double-particle-linkage model by Lan et al. (2017). Study of dynamics near the mass dipole model was started by Chermnykh (1987), where the stability of the libration points was investigated. The corresponding problem is named the Chermnykh problem and study on the stability of libration points was extended by Goździewski (1998). Prieto-Llanos & Gomez-Tierno (1994) also applied this model for the Mars-Phobos system. Recently, Zeng et al. (2017) extended the dipole model to the case that both primaries have oblateness. An important advantage of the mass dipole model is that it connects the dynamics of near elongated asteroids with the dynamics of the circular restricted three-body problem.

Application of the mass dipole model (i.e. the double-particle-linkage model) is based on an important assumption that an elongated asteroid has an approximately axisymmetric shape about the $x$ axis. This assumption is reasonable for asteroids such as 216 Kleopatra, 951 Gaspra and 1620 Geographos. However, it no longer holds true for some elongated asteroids (e.g. 243 Ida) which have arched shapes. In order to solve this problem, Lan et al. (2017) proposed a triple-particle-linkage model based on the model of Zeng et al. (2015). In their proposed model, an external non-collinear primary is connected to the mass dipole model. Their model is axisymmetric about the $y$ axis which cannot reflect the non-uniformity of the mass distribution for non-axisymmetric elongated asteroids. To overcome this issue, one effective way is to use the mascon gravitation model which can be regarded as a multiple particle-linkage model. In the work of Chanut et al. (2015), a mascon gravitational model based on the polyhedral model was proposed. However, the computational time increases with the number of mass particles. Moreover, it becomes difficult to analyze the effect of the mass distribution on the dynamics due to the large number of parameters. Therefore, we aim to improve the simplified particle-linkage models (Zeng et al. 2015; Lan et al. 2017).

In the current work, non-axisymmetric elongated asteroids are investigated. A non-axisymmetric triple-particle-linkage model is proposed to achieve improved performance over both the double-particle-linkage model (i.e. the mass dipole model) and the axisymmetric triple-particle-linkage model for target elongated asteroids. This paper also aims to propose a method based on nonlinear optimization for parameter determination of the simplified model. This method has the advantage of reducing the total position error for the equilibrium points compared with the previous method (Zeng et al. 2015) where only the equilibrium point with maximum deviation was considered. In addition, the proposed simplified model is compared to the polyhedral method in terms of both topological classification of the equilibrium points and distribution of gravitational errors for justification of the simplified model.

The advantages of the studied model are as follows. First, this model has better approximation performance than the two previous particle-linkage models (Zeng et al. 2015; Lan et al. 2017) for connecting with the precision model (i.e. polyhedral model) of non-axisymmetric elongated asteroids. Second, it is beneficial for qualitatively analyzing the effects of model parameters although the studied model is only an approximate model. Qualitative analyses can analyze the effects of a few mass distribution parameters in the following aspects: the variation tendency of required control for body-fixed hovering (Yang et al. 2015), shapes and distributions of the linearly stable body-fixed hovering regions (Yang et al. 2015), the width and distribution of stable periodic orbits near the equatorial plane (Lan et al. 2017), etc. Moreover, based on qualitative analyses, it has the potential to guide control design with the precision model. For example, linear feedback control for body-fixed hovering control is designed for elongated asteroids based on characteristics of the double-particle-linkage model (Yang et al. 2017). Third, the simplified model also can be used for estimating the magnitude level of required control for maneuvers (e.g. body-fixed hovering).

The paper is organized as follows. The normalized equation of motion near asteroids and two existing particle-linkage models are introduced in Section 2.

Thereafter, the non-axisymmetric triple-particle-linkage model is proposed based on these existing models to serve as the simplified model. In Section 3, a method for determining the parameters of the simplified model based on nonlinear optimization is given. In Section 4, The proposed model and method are applied for three non-axisymmetric elongated asteroids, 243 Ida, 433 Eros and (8567) 1996 HW1 (hereafter called 1996 HW1). The performance of the current model is compared with the two existing models to show the advantage of reducing the matching error. In Section 5, the rationality of the simplified model is further verified by topological classification of equilibrium points and the distribution of gravitational potential. Section 6 gives the conclusion of the paper.

## 2 DYNAMICAL MODEL

In this section, the motion equations near an elongated asteroid are derived. Thereafter, two axisymmetric particle-linkage models approximating the gravitational field of the asteroid are introduced. Last, an improved approximate simple model, which is a non-axisymmetric particle-linkage model, is presented.

### 2.1 Equations of Motion

The motion of a massless particle in the gravitational field of a uniformly rotating non-axisymmetric elongated asteroid is considered. A body-fixed frame, for which the origin is at the center of mass of the asteroid and the three axes are aligned with the three principle axes of the asteroid, is adopted. The equation of motion in this frame is

$$\ddot{\boldsymbol{r}} + 2\boldsymbol{\omega} \times \dot{\boldsymbol{r}} + \boldsymbol{\omega} \times (\boldsymbol{\omega} \times \mathbf{r}) + \boldsymbol{g} = 0\,, \tag{1}$$

where $\boldsymbol{r} = [x, y, z]^{\mathrm{T}}$ represents the position vector of the particle relative to the mass center, $\boldsymbol{\omega} = [0, 0, \omega]^{\mathrm{T}}$ denotes the angular velocity vector and $\boldsymbol{g}$ is the gravitational acceleration which is

$$\boldsymbol{g} = \left[\begin{array}{ccc} \frac{\partial U}{\partial x} & \frac{\partial U}{\partial y} & \frac{\partial U}{\partial z} \end{array}\right]^{\mathrm{T}}. \tag{2}$$

Here $U$ is the gravitational potential. The definition of $U$ herein is

$$U = -G \iiint\limits_{\mathrm{body}} \frac{1}{r} dm\,, \tag{3}$$

where $G$ is the gravitational constant, $r$ is the distance relative to the origin and $m$ is the mass of a mass point on the asteroid.

Defining the effective potential as (Yang et al. 2015; Zeng et al. 2015; Lan et al. 2017)

$$V = -\frac{1}{2}(\boldsymbol{\omega} \times \boldsymbol{r}) \cdot (\boldsymbol{\omega} \times \boldsymbol{r}) + U\,, \tag{4}$$

we can rewrite Equation (1) as

$$\ddot{\boldsymbol{r}} + 2\boldsymbol{\omega} \times \dot{\boldsymbol{r}} + \frac{\partial V}{\partial \boldsymbol{r}} = 0\,. \tag{5}$$

Selecting the length unit as $L$ and the time unit as $\omega^{-1}$, we can rewrite Equation (5) in a normalized form (Yang et al. 2017)

$$\begin{cases} \hat{x}'' - 2\hat{y}' + \hat{V}_x = 0\,, \\ \hat{y}'' + 2\hat{x}' + \hat{V}_y = 0\,, \\ \hat{z}'' + \hat{V}_z = 0\,, \end{cases} \tag{6}$$

where $\hat{a}$ represents the normalized form of $a$, $a'$ and $a''$ denote the first and second order derivatives of $a$ respectively, and the subscripts $x$, $y$ and $z$ signify the partial derivatives with respect to the position.

### 2.2 Existing Particle-Linkage Models

In this part, two axisymmetric particle-linkage models which have been proposed by prior studies are briefly introduced.

The first axisymmetric particle-linkage model is the double-particle-linkage model which is known as the mass dipole model (Zeng et al. 2015). As shown in Figure 1(a), this model is composed of two particles and a massless rod. The masses of the two particles are $M_1$ and $M_2$ and the total mass is $M$. The length between these two particles is $L$. Denote a mass ratio $\mu = M_1/M$. Then, the normalized positions of these particles are $\hat{x}_{M_1} = 1 - \mu$, $\hat{x}_{M_2} = \mu$ and $\hat{y}_{M_1} = \hat{y}_{M_2} = \hat{z}_{M_1} = \hat{z}_{M_2} = 0$.

For this model, the effective potential is (Yang et al. 2015; Zeng et al. 2015)

$$\hat{V} = -\frac{\hat{x}^2 + \hat{y}^2}{2} - k\left(\frac{\mu}{\hat{r}_1} + \frac{1-\mu}{\hat{r}_2}\right)\,, \tag{7}$$

where

$$\hat{r}_1 = \sqrt{(\hat{x} - \hat{x}_{M_1})^2 + (\hat{y} - \hat{y}_{M_1})^2}\,,$$

$$\hat{r}_2 = \sqrt{(\hat{x} - \hat{x}_{M_2})^2 + (\hat{y} - \hat{y}_{M_2})^2},$$

and the dimensionless parameter $k$ is

$$k = \frac{GM}{\omega^2 L^3}\,. \tag{8}$$

The elements of the gradient of the effective potential are

$$\hat{V}_x = -\hat{x} + k\left[\frac{\mu}{\hat{r}_1^3}\left(\hat{x} - \hat{x}_{M_1}\right) + \frac{1-\mu}{\hat{r}_2^3}\left(\hat{x} - \hat{x}_{M_2}\right)\right], \tag{9}$$

$$\hat{V}_y = -\hat{y} + k\left[\frac{\mu}{\hat{r}_1^3}\left(\hat{y} - \hat{y}_{M_1}\right) + \frac{1-\mu}{\hat{r}_2^3}\left(\hat{y} - \hat{y}_{M_2}\right)\right], \tag{10}$$

$$\hat{V}_z = -\hat{z} + k\left[\frac{\mu}{\hat{r}_1^3}\left(\hat{z} - \hat{z}_{M_1}\right) + \frac{1-\mu}{\hat{r}_2^3}\left(\hat{z} - \hat{z}_{M_2}\right)\right]. \tag{11}$$

According to Figure 1(a), the double-particle-linkage model is symmetric about the $x$ axis. In the study of Zeng et al. (2015), it is shown that this model has good accuracy for an elongated asteroid when its mass distribution is approximately symmetric about the $x$ axis. However, some elongated asteroids, such as asteroid 243 Ida (as shown in Fig. 1), have an arched shape. In order to study these asteroids, Lan et al. (2017) proposed a particle-linkage model which is not symmetric about the $x$ axis and also has only few design parameters, similar to the double-particle-linkage model.

The second particle-linkage model is the axisymmetric triple-particle-linkage model (Lan et al. 2017) as shown in Figure 1(b). This model is composed of three particles and two massless rods. The masses of the three particles are $M_1$, $M_1$ and $M_2$ and the total mass is $M$. The relative positions of these particles are illustrated in Figure 1(b). Denote a mass ratio $\mu = M_1/M$ and length ratio $\sigma = h/L$. Then, the normalized positions of these particles are

$$\begin{cases} \hat{x}_1 = -\frac{1}{2}, \quad \hat{y}_1 = (1-2\mu)\,\sigma, \quad \hat{z}_1 = 0\,, \\ \hat{x}_2 = \frac{1}{2}, \quad \hat{y}_2 = (1-2\mu)\,\sigma, \quad \hat{z}_2 = 0\,, \\ \hat{x}_3 = 0, \quad \hat{y}_3 = 2\mu\sigma, \quad \hat{z}_3 = 0\,. \end{cases} \tag{12}$$

For this model, the effective potential is

$$\hat{V} = -\frac{\hat{x}^2 + \hat{y}^2}{2} - k\left(\frac{\mu}{\hat{r}_1} + \frac{\mu}{\hat{r}_2} + \frac{1-2\mu}{\hat{r}_3}\right), \tag{13}$$

where

$$\hat{r}_1 = \sqrt{\left(\hat{x} - \hat{x}_1\right)^2 + \left(\hat{y} - \hat{y}_1\right)^2}\,,$$

$$\hat{r}_2 = \sqrt{\left(\hat{x} - \hat{x}_2\right)^2 + \left(\hat{y} - \hat{y}_2\right)^2}\,,$$

and

$$\hat{r}_3 = \sqrt{\left(\hat{x} - \hat{x}_3\right)^2 + \left(\hat{y} - \hat{y}_3\right)^2}\,.$$

The elements of the gradient of the effective potential are

$$\hat{V}_x = -\,\hat{x} + k\left[\frac{\mu}{\hat{r}_1^3}\left(\hat{x} - \hat{x}_1\right) + \frac{\mu}{\hat{r}_2^3}\left(\hat{x} - \hat{x}_2\right) + \frac{1-2\mu}{\hat{r}_3^3}\left(\hat{x} - \hat{x}_3\right)\right], \tag{14}$$

$$\hat{V}_y = -\,\hat{y} + k\left[\frac{\mu}{\hat{r}_1^3}\left(\hat{y} - \hat{y}_1\right) + \frac{\mu}{\hat{r}_2^3}\left(\hat{y} - \hat{y}_2\right) + \frac{1-2\mu}{\hat{r}_3^3}\left(\hat{y} - \hat{y}_3\right)\right], \tag{15}$$

$$\hat{V}_z = -\,\hat{z} + k\left[\frac{\mu}{\hat{r}_1^3}\left(\hat{z} - \hat{z}_1\right) + \frac{\mu}{\hat{r}_2^3}\left(\hat{z} - \hat{z}_2\right) + \frac{1-2\mu}{\hat{r}_2^3}\left(\hat{z} - \hat{z}_3\right)\right]. \tag{16}$$

Although this model is not symmetric about the $x$ axis, it is symmetric about the $y$ axis. However, some elongated asteroids, such as 243 Ida and 433 Eros, are not very approximately symmetric about the $y$ axis. There is still room for improvement in the accuracy of this axisymmetric triple-particle-linkage model. Therefore, a non-axisymmetric triple-particle-linkage model is proposed which is presented in the next subsection.

### 2.3 Non-Axisymmetric Triple-Particle-Linkage Model

A schematic diagram of the non-axisymmetric triple-particle-linkage model is shown in Figure 2. From this figure, it can be seen that this model is also composed of three particles and two massless rods. It is assumed that particles $M_1$ and $M_2$ are located on the $x_1$ axis, which is parallel to the $x$ axis. The distance between these two particles is denoted as $L$. In addition, the deviations of the third particle $M_3$ relative to the center of the rod which connects $M_1$ and $M_2$ are $l_1$ and $l_2$ along the $x$ and $y$ axes, respectively.

In order to derive the normalized effective potential, the mass ratios of these three particles to the total mass $M$ are denoted as $\mu_1$, $\mu_2(1-\mu_1)$ and $(1-\mu_2)(1-\mu_1)$. Besides, two dimensionless parameters are defined to describe the deviation of $M_3$ which are $\sigma_1 = l_1/L$ and $\sigma_2 = l_2/L$. Thereafter, the positions of $M_1$, $M_2$ and $M_3$ in the frame $o_1 - x_1y_1z_1$ are $[-1/2, 0, 0]$, $[1/2, 0, 0]$ and $[\sigma_1, \sigma_2, 0]$ respectively. The positions of these particles in the frame *o-xyz* which is centered at the center of mass of the model are as follows:

$$\begin{cases} \hat{x}_{M_1} = -\frac{1}{2} + \frac{\mu_1}{2} - \frac{\mu_2(1-\mu_1)}{2} - \frac{(1-\mu_2)(1-\mu_1)}{2}\sigma_1\,, \\ \hat{y}_{M_1} = -\frac{(1-\mu_2)(1-\mu_1)}{2}\sigma_2\,, \\ \hat{z}_{M_1} = 0\,. \end{cases} \tag{17}$$

$$\begin{cases} \hat{x}_{M_2} = \frac{1}{2} + \frac{\mu_1}{2} - \frac{\mu_2(1-\mu_1)}{2} - \frac{(1-\mu_2)(1-\mu_1)}{2}\sigma_1\,, \\ \hat{y}_{M_2} = -\frac{(1-\mu_2)(1-\mu_1)}{2}\sigma_2\,, \\ \hat{z}_{M_2} = 0\,. \end{cases} \tag{18}$$

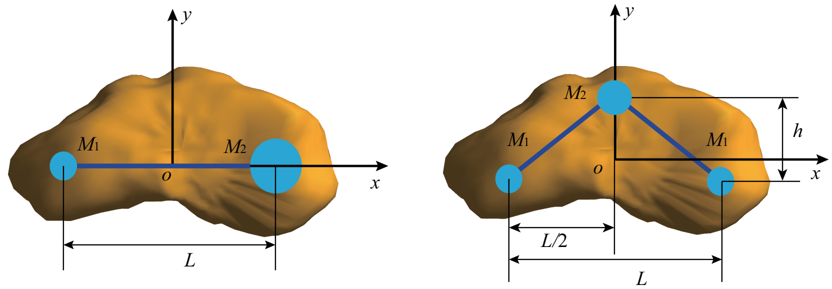


(a) Double-particle-linkage model (b) Axisymmetric triple-particle-linkage model

**Fig. 1** Axisymmetric particle-linkage models.

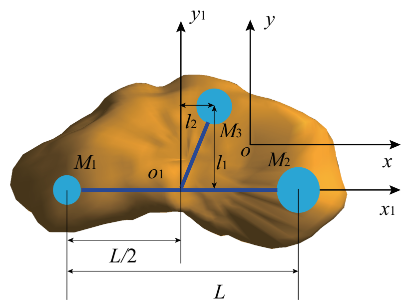


**Fig. 2** Non-axisymmetric triple-particle-linkage model.

$$\begin{cases} \hat{x}_{M_3} = \sigma_1 + \frac{\mu_1}{2} - \frac{\mu_2(1-\mu_1)}{2} - \frac{(1-\mu_2)(1-\mu_1)}{2}\sigma_1\,, \\ \hat{y}_{M_3} = \frac{(1-\mu_2)(1-\mu_1)}{2}\sigma_2\,, \\ \hat{z}_{M_3} = 0\,. \end{cases} \tag{19}$$

For this model, the effective potential is

$$\begin{aligned} \hat{V} = & -\frac{\hat{x}^2+\hat{y}^2}{2} - k\left[\frac{\mu_1}{\hat{r}_1} + \frac{\mu_2(1-\mu_1)}{\hat{r}_2}\right. \\ & \left. + \frac{(1-\mu_2)(1-\mu_1)}{\hat{r}_3}\right]\,, \end{aligned} \tag{20}$$

where

$$\hat{r}_1 = \sqrt{(\hat{x}-\hat{x}_{M_1})^2 + (\hat{y}-\hat{y}_{M_1})^2}\,,$$

$$\hat{r}_2 = \sqrt{(\hat{x}-\hat{x}_{M_2})^2 + (\hat{y}-\hat{y}_{M_2})^2}\,,$$

and

$$\hat{r}_3 = \sqrt{(\hat{x}-\hat{x}_{M_3})^2 + (\hat{y}-\hat{y}_{M_3})^2}\,.$$

The elements of the gradient of the effective potential are

$$\begin{aligned} \hat{V}_x = & -\hat{x} + k\left[\frac{\mu_1}{\hat{r}_1^3}(\hat{x}-\hat{x}_{M_1})\right. \\ & + \frac{\mu_2(1-\mu_1)}{\hat{r}_2^3}(\hat{x}-\hat{x}_{M_2}) \\ & \left. + \frac{(1-\mu_2)(1-\mu_1)}{\hat{r}_3^3}(\hat{x}-\hat{x}_{M_3})\right]\,, \end{aligned} \tag{21}$$

$$\begin{aligned} \hat{V}_y = & -\hat{y} + k\left[\frac{\mu_1}{\hat{r}_1^3}(\hat{y}-\hat{y}_{M_1})\right. \\ & + \frac{\mu_2(1-\mu_1)}{\hat{r}_2^3}(\hat{y}-\hat{y}_{M_2}) \\ & \left. + \frac{(1-\mu_2)(1-\mu_1)}{\hat{r}_3^3}(\hat{y}-\hat{y}_{M_3})\right]\,, \end{aligned} \tag{22}$$

$$\begin{aligned} \hat{V}_z = & k\left[\frac{\mu_1}{\hat{r}_1^3}\hat{z} + \frac{\mu_2(1-\mu_1)}{\hat{r}_2^3}\hat{z}\right. \\ & \left. + \frac{(1-\mu_2)(1-\mu_1)}{\hat{r}_3^3}\hat{z}\right]\,. \end{aligned} \tag{23}$$

## 3 PARAMETER DETERMINATION FOR THE NON-SYMMETRICAL TRIPLE-PARTICLE-LINKAGE MODEL

Three different particle-linkage models have been presented in the preceding section. However, each particle-linkage model has unknown parameters that need to be determined. In this study, the angular velocity and total mass of each simplified model are set to be equivalent to those of the asteroid. Therefore, the double-particle-linkage model only has two unknown parameters which are $L$ and $\mu$. As for the axisymmetric triple-particle-linkage model, it has three unknown parameters which are $L$, $\sigma$ and $\mu$. The most complex model is the nonsymmetrical triple-particle-linkage model. It has five unknown parameters which are $L$, $\sigma_1$, $\sigma_2$, $\mu_1$ and $\mu_2$.

In this study, the parameters are determined by the positions of equilibrium points, similar to the approach used by Zeng et al. (2015). The position of an equilibrium point $[\hat{x}_E, \hat{y}_E, \hat{z}_E]$ satisfies the following equation

$$\begin{aligned}\hat{V}_x\left(\hat{x}_E, \hat{y}_E, \hat{z}_E\right) &= \hat{V}_y\left(\hat{x}_E, \hat{y}_E, \hat{z}_E\right) \\ &= \hat{V}_z\left(\hat{x}_E, \hat{y}_E, \hat{z}_E\right) = 0\,.\end{aligned} \tag{24}$$

The idea of Zeng et al. (2015) is to match the positions of equilibrium points from the simplified models with those of a precision model. But different from the work of Zeng et al. (2015), the total position matching error of all equilibrium points is minimized and the selected design approach in the current work is nonlinear optimization.

The method of parameter determination for the nonsymmetrical triple-particle-linkage model is as follows.

The optimization variables for this model are $X = [L, \sigma_1, \sigma_2, \mu_1, \mu_2]$. Both the upper bounds $[L_{\max}, \sigma_{1\max}, \sigma_{2\max}, \mu_{1\max}, \mu_{2\max}]$ and lower bounds $[L_{\min}, \sigma_{1\min}, \sigma_{2\min}, \mu_{1\min}, \mu_{2\min}]$ are set to get the constraints for each variable before optimization.

The performance index for the nonlinear optimization is chosen as

$$J_0 = \sum_{i=1}^{n} \sqrt{\left(\hat{x}_{Ei}L - x_{Ei}{}^{*}\right)^2 + \left(\hat{y}_{Ei}L - y_{Ei}{}^{*}\right)^2 + \left(z_{Ei}{}^{*}\right)^2}\,, \tag{25}$$

where $[\hat{x}_{Ei}, \hat{y}_{Ei}, \hat{z}_{Ei}]$ represents the normalized positions of the equilibrium points in the simplified models, $[x_{Ei}{}^{*}, y_{Ei}{}^{*}, z_{Ei}{}^{*}]$ corresponds to accurate positions of the equilibrium points, the subscript $i$ indicates the $i$th equilibrium point and $n$ represents the total number of equilibrium points. The total number of equilibrium points outside of elongated asteroids is usually four according to results in the work Wang et al. (2014). Moreover, accurate positions of the equilibrium points are computed by the polyhedral method of Werner & Scheeres (1996). Minimization of the performance index can be obtained by nonlinear optimization solvers (e.g. *fmincon* in MATLAB).

Determinations of parameters in the two axisymmetric models can be regarded as simplified cases of the non-axisymmetric model. The optimized variables should be modified to $X = [L, 0, 0, \mu, 1]$ for the double-particle-linkage model while they should be $X = [L, 0, \sigma, \mu, \mu/(1\text{-}\mu)]$ for the axisymmetric triple-particle-linkage model.

## 4 APPLICATION TO REALISTIC ELONGATED ASTEROIDS

In this section, the aforementioned particle-linkage models are applied to three realistic elongated asteroids, 243 Ida, 433 Eros and 1996 HW1, by the proposed parameter determination method. The improved performance of the axisymmetric triple-particle-linkage model compared with the double-particle-linkage model and the axisymmetric triple-particle-linkage model is also demonstrated.

### 4.1 Parameters of the Sample Elongated Asteroids

The bulk densities and rotation periods of the three elongated asteroids are listed in Table 1. In this study, the polyhedral models are regarded as the precision model and the polyhedral method (Werner & Scheeres 1996) is used to compute accurate gravitational potentials for the asteroids. The used data for the polyhedral models of these asteroids are also given in Table 1. The masses of the asteroids are obtained by the polyhedral models.

By using the polyhedral method, accurate positions of the equilibrium points for Equation (25) are obtained. The results are shown in Table 2. It should be pointed out that only the equilibrium points outside of each asteroid are considered.

In simulations, the boundary constraints for each particle-linkage model are chosen as follows:

(1) Non-axisymmetric triple-particle-linkage model: $[L_{\max}, L_{\min}]$ are set to [30, 60] km, [20, 40] km and [1, 4] km for 243 Ida, 433 Eros and 1996 HW1, respectively. $[\sigma_{1\min}, \sigma_{1\max}]$ are set to [–0.5, 0.5] for each asteroid. $[\sigma_{2\min}, \sigma_{2\max}]$ are set to [–0.2, 0.2] for 243 Ida and 433 Eros and [–0.4, 0.4] for 1996 HW1. $[\mu_{1\min}, \mu_{1\max}]$ and $[\mu_{2\min}, \mu_{2\max}]$ are both set to [0.001, 0.999] for each asteroid.
(2) Axisymmetric triple-particle-linkage model: $[L_{\max}, L_{\min}]$ are set to [30, 60] km, [20, 40] km and [1, 4] km for 243 Ida, 433 Eros and 1996 HW1, respectively. $[\sigma_{\min}, \sigma_{\max}]$ are all set to [–0.3, 0.3]. $[\mu_{\min}, \mu_{\max}]$ are all set to [0.001, 0.499].
(3) Double-particle-linkage model: $[L_{\max}, L_{\min}]$ are set to [20, 60] km, [15, 40] km and [1, 4] km for 243 Ida, 433 Eros and 1996 HW1, respectively. $[\mu_{\min}, \mu_{\max}]$ are all set to [0.001, 0.999].

The process of selecting these boundary constraints is as follows. As for the geometry parameters $L$, $\sigma_1$, $\sigma_2$ and $\sigma$, the boundary constraints are set according to the actual shapes of the asteroids. If the value of a geometry

**Table 1** Physical and Polyhedral Parameters of the Asteroids

| Asteroid | Bulk density[a] ($\mathrm{g\,cm^{-3}}$) | Rotation period (h) | $M$ (kg) | Vertices & Facets[bcd] |
|---|---|---|---|---|
| 243 Ida | 2.6 | 4.63 | $4.077860\times 10^{16}$ | 2522 & 5040 |
| 433 Eros | 2.67 | 5.27 | $6.652614 \times 10^{15}$ | 856 & 1708 |
| 1996 $HW_1$ | 3.56 | 8.757 | $1.543656 \times 10^{13}$ | 1392 & 2780 |

Notes: [a] Wang et al. (2014); [b] Stooke (2016); [c]Thomas et al. (2001); [d]Magri et al. (2017).

**Table 2** Positions of Equilibrium Points for the Asteroids

| Asteroid | E1 (km) | E2 (km) | E3 (km) | E4 (km) |
|---|---|---|---|---|
| 243 Ida | [31.3950, –5.9630, 0.0340] | [–1.4150, 25.4106, –0.3786] | [–33.3547, –4.8504, –1.0886] | [–2.1609, –23.5709, 0.0975] |
| 433 Eros | [19.1304, –2.6118, 0.1414] | [0.4717, 14.6974, –0.0615] | [–19.6938, –3.3419, 0.1218] | [–0.4475, –13.9483, –0.0734] |
| 1996 HW1 | [3.2117, 0.1338, –0.0023] | [–0.1501, 2.8076, 0.0005] | [–3.2684, 0.0841, –0.0010] | [–0.1811, –2.8258, 0.0001] |

**Table 3** Optimization Results for the Double-particle-linkage Model

| Asteroid | $L$ (km) | $\mu$ | $k$ | $J_0$ (km) | $J_1$ | $J_2$ |
|---|---|---|---|---|---|---|
| 243 Ida | 25.0886 | 0.4155 | 1.2126 | 13.1781 | 23.8853% | 0.4820% |
| 433 Eros | 15.3094 | 0.4764 | 1.1279 | 7.2729 | 22.2942% | 0.7634% |
| 1996 HW1 | 1.8736 | 0.4194 | 3.9426 | 0.0812 | 2.2471% | 0.0195% |

parameter is at the boundary after the optimization, we enlarge its range and conduct optimization again to make the optimized parameter be located between the boundaries. As for the mass ratios, the boundary constraints are set according to their theoretical ranges.

The initial guesses for each particle-linkage model are chosen as follows:

(1) Non-axisymmetric triple-particle-linkage model: [$L$, $\sigma_1$, $\sigma_2$, $\mu_1$, $\mu_2$] are set to [40, 0.0, 0.2, 0.5, 0.5], [30, 0.0, 0.2, 0.5, 0.5] and [2, 0.0, 0.0, 0.5, 0.5], respectively.
(2) Axisymmetric triple-particle-linkage model: [$L$, $\sigma$, $\mu$] are set to [40, 0.2, 0.4], [30, 0.2, 0.4] and [2, 0.2, 0.4], respectively.
(3) Double-particle-linkage model: [$L$, $\mu$] are set to [40, 0.5], [30, 0.5] and [2, 0.5], respectively.

### 4.2 Optimization Results for the Particle-Linkage Models

By application of the optimization method mentioned in Section 3, the optimization results of the three particle-linkage models are obtained as shown in Tables 3 – 5. In these tables, definitions of the performance indexes $J_1$ and $J_2$ are as follows:

$$J_1 = \max\left(\frac{\sqrt{(\hat{x}_{Ei}L - x_{Ei}{}^*)^2 + (\hat{y}_{Ei}L - y_{Ei}{}^*)^2 + (z_{Ei}{}^*)^2}}{L} \times 100\%\right), \qquad i = 1, 2, 3, 4\,, \tag{26}$$

$$J_2 = \min\left(\frac{\sqrt{(\hat{x}_{Ei}L - x_{Ei}{}^*)^2 + (\hat{y}_{Ei}L - y_{Ei}{}^*)^2 + (z_{Ei}{}^*)^2}}{L} \times 100\%\right), \qquad i = 1, 2, 3, 4\,. \tag{27}$$

These performance indexes are computed after optimal parameters for the index $J_0$ have been obtained. They indicate the maximum and minimum relative errors for a single equilibrium point, respectively.

Comparing the data in these tables and results in the studies of Zeng et al. (2015) and Lan et al. (2017), we find the following properties and results:

From Table 3, it can be found that the double-particle-linkage model is not suitable for asteroids 243 Ida and 433 Eros because the maximum relative errors are both over 20.0%. In fact, these two asteroids are

**Table 4** Optimization Results for the Axisymmetric Triple-particle-linkage Model

| Asteroid | $L$ (km) | $\sigma$ | $\mu$ | $k$ | $J_0$ (km) | $J_1$ | $J_2$ |
|---|---|---|---|---|---|---|---|
| 243 Ida | 33.7302 | 0.2097 | 0.2465 | 0.4990 | 6.3052 | 6.7963% | 0.7076% |
| 433 Eros | 21.0353 | 0.1717 | 0.2601 | 0.4348 | 2.1849 | 3.5865% | 1.3244% |
| 1996 HW1 | 2.0174 | –0.2596 | 0.4434 | 3.1580 | 0.1409 | 3.1797% | 0.4126% |

**Table 5** Optimization Results for the Non-axisymmetric Triple-particle-linkage Model

| Asteroid | $L$ (km) | $\sigma_1$ | $\sigma_2$ | $\mu_1$ | $\mu_2$ | $k$ | $J_0$ (km) | $J_1$ | $J_2$ |
|---|---|---|---|---|---|---|---|---|---|
| 243 Ida | 37.1096 | 0.0500 | 0.1719 | 0.1893 | 0.3132 | 0.3747 | 1.9082 | 3.0860% | 0.1038% |
| 433 Eros | 21.3237 | 0.0074 | 0.1604 | 0.2373 | 0.3597 | 0.4174 | 1.6342 | 3.7642% | 0.3464% |
| 1996 HW1 | 1.9931 | 0.0913 | –0.3929 | 0.4014 | 0.9097 | 3.2749 | 0.0183 | 0.6936% | 0.0089% |

**Table 6** Topological Classification and Stability of Equilibrium Points

| Topological classification | Forms of eigenvalues | Stability |
|---|---|---|
| Case 1 | $\pm i\beta(\beta_j \in R^+; j = 1,2,3)$ | Linearly stable |
| Case 2 | $\pm\alpha_j(\alpha_j \in R^+; j = 1), \pm i\beta(\beta_j \in R^+; j = 1,2)$ | Unstable |
| Case 3 | $\pm\alpha_j(\alpha_j \in R^+; j = 1,2), \pm i\beta(\beta_j \in R^+; j = 1)$ | Unstable |
| Case 4a | $\pm\alpha_j(\alpha_j \in R^+; j = 1), \pm\sigma \pm i\tau(\sigma,\tau \in R^+)$ | Unstable |
| Case 4b | $\pm\alpha_j(\alpha_j \in R^+; j = 1,2,3)$ | Unstable |
| Case 5 | $\pm\sigma \pm i\tau(\sigma,\tau \in R^+), \pm i\beta(\beta_j \in R^+; j = 1)$ | Unstable |

not studied in the work of Zeng et al. (2015). However, the maximum relative error is only 2.2471% for asteroid 1996 HW1, which means this model is suitable for approximation. Moreover, this maximum relative error is smaller than the result of Zeng et al. (2015). The reason is due to the nonlinear optimization that is used in this study, which is considered to be a better procedure for determining the parameters.

Comparing Table 4 with Table 3, we see that the total errors and the maximum relative errors of the axisymmetric triple-particle-linkage model are much smaller than those of the double-particle-linkage model for asteroids 243 Ida and 433 Eros. Therefore, the external particle in the axisymmetric triple-particle-linkage model is important for reducing the model error. However, the axisymmetric triple-particle-linkage model has worse accuracy compared with the double-particle-linkage model for asteroid 1996 HW1. The camber of 1996 HW1 is much lower than those of 243 Ida and 433 Eros. Indeed, as mentioned above, this asteroid is studied by Zeng et al. (2015) using the double-particle-linkage model. Thus, the importance of the external mass becomes much lower. Moreover, because the mass distribution is symmetric along the $x$ axis for the axisymmetric triple-particle-linkage model, but it is not for the double-particle-linkage model, this indicates the asymmetry in the mass distribution along the $x$ axis is also an important factor for guaranteeing accuracy.

Comparing Table 5 with Tables 3 and 4, it can be concluded that the non-axisymmetric triple-particle-linkage model leads to the smallest total error $J_0$ for each asteroid. Therefore, the accuracy of the non-axisymmetric triple-particle-linkage model is better than that of existing particle-linkage models (Zeng et al. 2015; Lan et al. 2017). The maximum relative errors are only 3.0860%, 3.7642% and 0.6936% for these asteroids, respectively. Although the maximum relative error of the non-axisymmetric triple-particle-linkage model is slightly larger than the axisymmetric triple-particle-linkage model for 433 Eros, both the total error and the minimum relative error are smaller.

Consequently, the non-axisymmetric triple-particle-linkage model has advantages over the two existing particle-linkage models for matching equilibrium points of the polyhedral model.

## 5 COMPARISON BETWEEN THE SIMPLIFIED MODEL AND THE POLYHEDRAL MODEL

In the preceding section, the parameters of the non-axisymmetric triple-particle-linkage model were obtained. The position errors of the equilibrium points between this simplified model and the polyhedral model are small for our sample of elongated asteroids.

In this section, topological classifications of the equilibrium points and distributions of the gravitational potentials between the non-axisymmetric triple-particle-linkage model and the polyhedral model are compared for further justification of the non-axisymmetric triple-particle-linkage model.

### 5.1 Topological Classification of the Equilibrium Points

According to prior works (Jiang et al. 2014), the linearized motion near an equilibrium point can be written as

$$\begin{cases} \xi'' - 2\eta' + \hat{V}_{xx}\xi + \hat{V}_{xy}\eta + \hat{V}_{xz}\varsigma = 0\,, \\ \eta'' + 2\xi' + \hat{V}_{xy}\xi + \hat{V}_{yy}\eta + \hat{V}_{yz}\varsigma = 0\,, \\ \zeta'' + \hat{V}_{xz}\xi + \hat{V}_{yz}\eta + \hat{V}_{zz}\varsigma = 0\,, \end{cases} \tag{28}$$

where $\xi$, $\eta$ and $\zeta$ are position disturbances along each axis, respectively. The eigenvalues of the equation satisfy (Jiang et al. 2014)

$$\begin{aligned} &\lambda^6 + \left(\hat{V}_{xx} + \hat{V}_{yy} + \hat{V}_{zz} + 4\right)\lambda^4 \\ &\quad + \left(\hat{V}_{xx}\hat{V}_{yy} + \hat{V}_{yy}\hat{V}_{zz} + \hat{V}_{zz}\hat{V}_{xx} \right.\\ &\quad \left. - \hat{V}_{xy}^2 - \hat{V}_{yz}^2 - \hat{V}_{xz}^2 + 4\hat{V}_{zz}\right)\lambda^2 \\ &\quad + \left(\hat{V}_{xx}\hat{V}_{yy}\hat{V}_{zz} + 2\hat{V}_{xy}\hat{V}_{yz}\hat{V}_{xz} \right.\\ &\quad \left. - \hat{V}_{xx}\hat{V}_{yz}^2 - \hat{V}_{yy}\hat{V}_{xz}^2 - \hat{V}_{zz}\hat{V}_{xy}^2\right) = 0\,, \end{aligned} \tag{29}$$

where $\lambda$ represents the eigenvalues. The eigenvalues determine the manifolds and stability of motion near the equilibrium point. According to Jiang et al. (2014) and Wang et al. (2014), the topological classifications for non-degenerate and non-resonant equilibrium points have five cases which are classified based on the forms of the eigenvalues as shown in Table 6. The stability for each case is also given in this table. According to Table 6, only Case 1 leads to a linearly stable equilibrium point.

As for the non-axisymmetric triple-particle-linkage model, elements of the Hessian matrix of the effective potential are

$$\begin{aligned} \hat{V}_{xx} = -1 + k &\left[\frac{\mu_1}{\hat{r}_1^3} - \frac{3\mu_1}{\hat{r}_1^5}(\hat{x} - \hat{x}_{M_1})^2 \right.\\ &+ \frac{\mu_2(1-\mu_1)}{\hat{r}_2^3} - \frac{3\mu_2(1-\mu_1)}{\hat{r}_2^5}(\hat{x} - \hat{x}_{M_2})^2 \\ &\left. + \frac{(1-\mu_2)(1-\mu_1)}{\hat{r}_3^3} - \frac{(1-\mu_2)(1-\mu_1)}{\hat{r}_3^5}(\hat{x} - \hat{x}_{M_3})^2\right]\,, \end{aligned} \tag{30}$$

**Table 7** Results of Topological Classifications by the Simplified Model

| Asteroid | E1 | E2 | E3 | E4 |
|---|---|---|---|---|
| 243 Ida | Case 2 | Case 5 | Case 2 | Case 5 |
| 433 Eros | Case 2 | Case 5 | Case 2 | Case 5 |
| 1996 HW1 | Case 2 | Case 5 | Case 2 | Case 5 |

$$\begin{aligned} \hat{V}_{yy} = -1 + k &\left[\frac{\mu_1}{\hat{r}_1^3} - \frac{3\mu_1}{\hat{r}_1^5}(\hat{y} - \hat{y}_{M_1})^2 \right.\\ &+ \frac{\mu_2(1-\mu_1)}{\hat{r}_2^3}r - \frac{3\mu_2(1-\mu_1)}{\hat{r}_2^5}(\hat{y} - \hat{y}_{M_2})^2 \\ &\left. + \frac{(1-\mu_2)(1-\mu_1)}{\hat{r}_3^3} - \frac{(1-\mu_2)(1-\mu_1)}{\hat{r}_3^5}(\hat{y} - \hat{y}_{M_3})^2\right]\,, \end{aligned} \tag{31}$$

$$\begin{aligned} \hat{V}_{zz} = k &\left[\frac{\mu_1}{\hat{r}_1^3} - \frac{3\mu_1}{\hat{r}_1^5}\hat{z}^2 + \frac{\mu_2(1-\mu_1)}{\hat{r}_2^3} - \frac{3\mu_2(1-\mu_1)}{\hat{r}_2^5}\hat{z}^2 \right.\\ &\left. + \frac{(1-\mu_2)(1-\mu_1)}{\hat{r}_3^3} - \frac{(1-\mu_2)(1-\mu_1)}{\hat{r}_3^5}\hat{z}^2\right]\,, \end{aligned} \tag{32}$$

$$\begin{aligned} \hat{V}_{xy} = \hat{V}_{yx} = -3k &\left[\frac{\mu_1}{\hat{r}_1^5}(\hat{x} - \hat{x}_{M_1})(\hat{y} - \hat{y}_{M_1}) \right.\\ &+ \frac{\mu_2(1-\mu_1)}{\hat{r}_2^5}(\hat{x} - \hat{x}_{M_2})(\hat{y} - \hat{y}_{M_2}) \\ &\left. + \frac{(1-\mu_2)(1-\mu_1)}{\hat{r}_3^5}(\hat{x} - \hat{x}_{M_3})(\hat{y} - \hat{y}_{M_3})\right]\,, \end{aligned} \tag{33}$$

$$\begin{aligned} \hat{V}_{xz} = \hat{V}_{zx} = -3k\hat{z} &\left[\frac{\mu_1}{\hat{r}_1^5}(\hat{x} - \hat{x}_{M_1}) \right.\\ &+ \frac{\mu_2(1-\mu_1)}{\hat{r}_2^5}(\hat{x} - \hat{x}_{M_2}) \\ &\left. + \frac{(1-\mu_2)(1-\mu_1)}{\hat{r}_3^5}(\hat{x} - \hat{x}_{M_3})\right]\,, \end{aligned} \tag{34}$$

$$\begin{aligned} \hat{V}_{yz} = \hat{V}_{zy} = -3k\hat{z} &\left[\frac{\mu_1}{\hat{r}_1^5}(\hat{y} - \hat{y}_{M_1}) \right.\\ &+ \frac{\mu_2(1-\mu_1)}{\hat{r}_2^5}(\hat{y} - \hat{y}_{M_2}) \\ &\left. + \frac{(1-\mu_2)(1-\mu_1)}{\hat{r}_3^5}(\hat{y} - \hat{y}_{M_3})\right]\,. \end{aligned} \tag{35}$$

With the optimized parameters in Table 5, the eigenvalues can be computed. Thereafter, the corresponding topological classifications for equilibrium points of the three sample asteroids are obtained as shown in Table 7. These topological cases are the same as those in the work of Wang et al. (2014) where the polyhedral model is used. Consequently, the topological cases of the equilibrium points are not changed by using the non-axisymmetric triple-particle-linkage model.

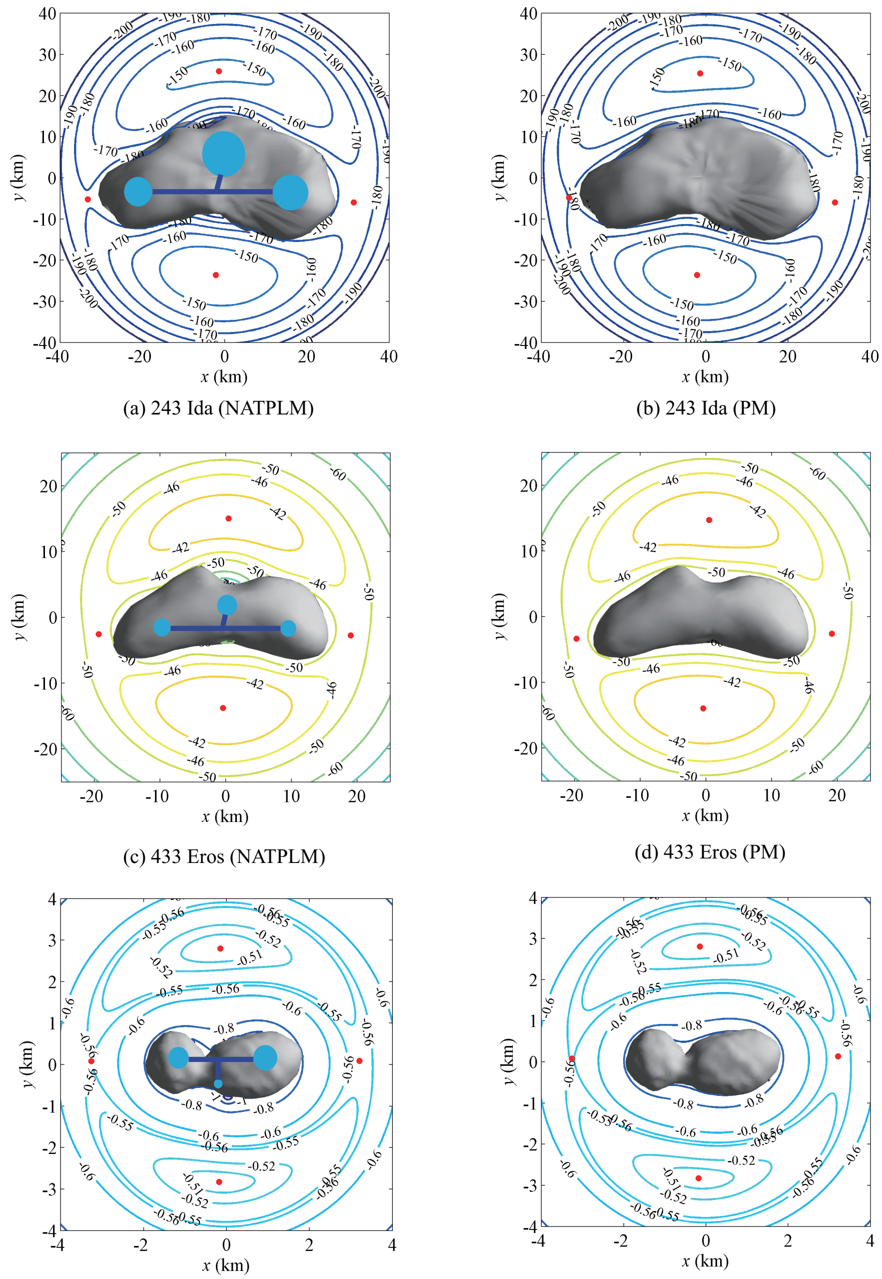

(a) 243 Ida (NATPLM) (b) 243 Ida (PM)

(c) 433 Eros (NATPLM) (d) 433 Eros (PM)

(e) 1996 HW1 (NATPLM) (f) 1996 HW1 (PM)

**Fig. 3** Distribution of the effective potentials near the asteroids (unit: $\mathrm{m^2\,s^{-2}}$). NATPLM represents the non-axisymmetric triple-particle-linkage model; PM signifies the polyhedral model. The *red points* stand for equilibrium points.

## 5.2 Distribution and Relative Errors of the Potentials

Thus far, it has been verified that position errors of the equilibrium points are small and the topological cases remain the same by application of the non-axisymmetric triple-particle-linkage model for the sample asteroids.

Next, we compare distributions of the effective potential and the gravitational potential between the non-axisymmetric triple-particle-linkage model and the polyhedral model for justification of this simplified model.

The distributions of effective potential for 243 Ida, 433 Eros and 1996 HW1 are shown in Figure 3, where subfigures (a), (c) and (e) are obtained by the non-axisymmetric triple-particle-linkage model and subfigures (b), (d) and (f) are obtained by the polyhedral model.

From Figure 3, it can be seen that each equilibrium point obtained by the non-axisymmetric triple-particle-

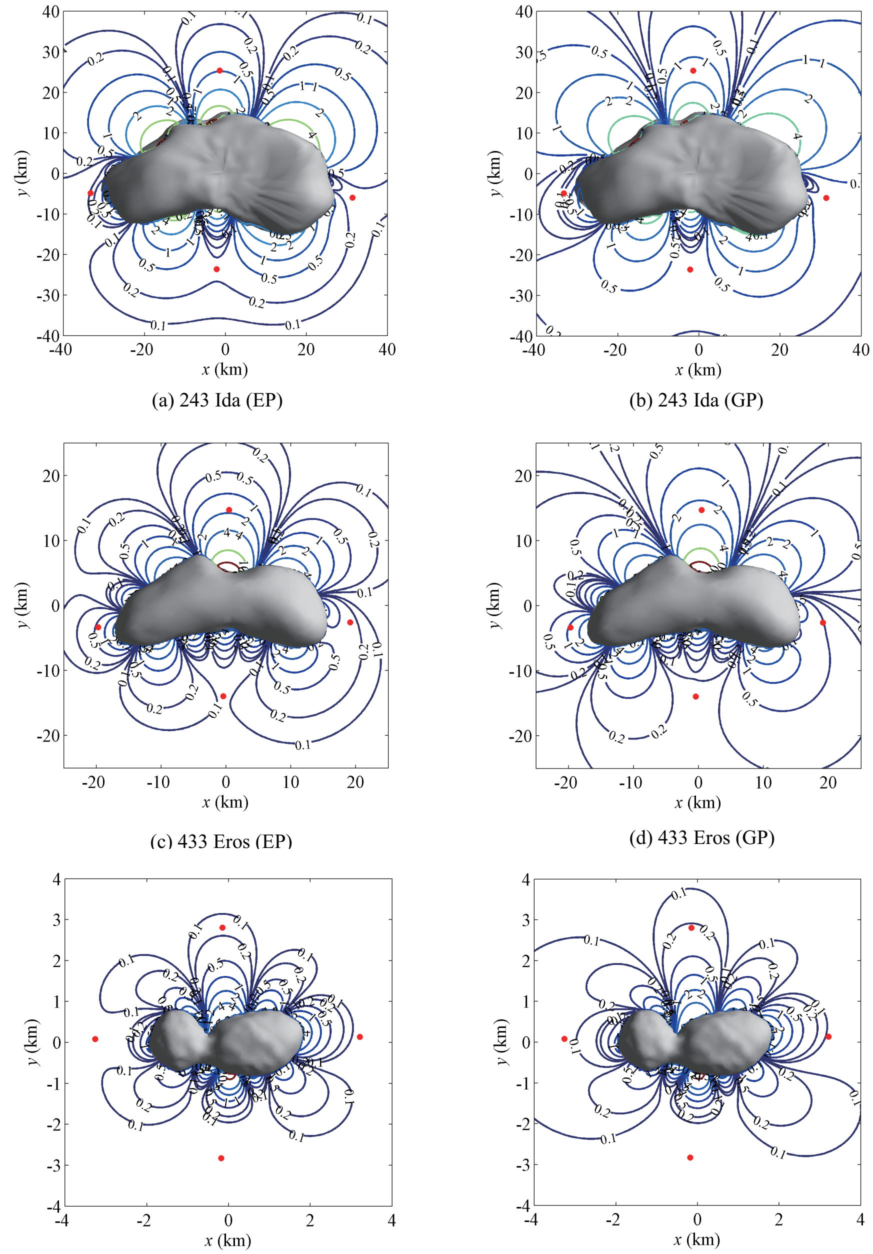

(a) 243 Ida (EP) (b) 243 Ida (GP)

(c) 433 Eros (EP) (d) 433 Eros (GP)

(e) 1996 HW1 (EP) (f) 1996 HW1 (GP)

**Fig. 4** Distribution of percentage errors for potentials near the asteroids. EP represents effective potential and GP signifies gravitational potential. The *red points* stand for equilibrium points.

linkage model has almost the same position as the corresponding equilibrium point obtained by the polyhedral model for each asteroid. Moreover, the distributions of the effective potential are very close when comparing (a) and (b), (c) and (d), and (e) and (f). These results indicate that the non-axisymmetric triple-particle-linkage model is a good approximation of the polyhedral model in the sense of distribution of the effective potential.

The relative errors of the effective potential and gravitational potential are further computed for verifying the accuracy of the non-axisymmetric triple-particle-linkage model. These relative errors, $E_V$ and $E_U$, are computed by

$$
\begin{aligned}
E_V &= \left|\frac{V_{\rm NATPLM} - V_{\rm PM}}{V_{\rm PM}}\right| \times 100\%, \\
E_U &= \left|\frac{U_{\rm NATPLM} - U_{\rm PM}}{U_{\rm PM}}\right| \times 100\%,
\end{aligned}
\qquad (36)
$$

where the subscripts 'NATPLM' and 'PM' represent the non-axisymmetric triple-particle-linkage model and the polyhedral model, respectively.

The results are shown in Figure 4, where subfigures (a), (c) and (e) represent the relative error of the effective potential and subfigures (b), (d) and (f) represent the relative error of the gravitational potential.

According to this figure, the relative errors are larger than 4% at only a small area near the surface of the asteroids. These relative errors are almost less than 2% beyond the equilibrium points for these asteroids. In such areas, the errors are even less than 0.2% for 1996 HW1. These results also support that the proposed simplified model approximates the non-axisymmetric elongated asteroids well.

## 6 CONCLUSIONS

This paper presents a simplified model for non-axisymmetric elongated asteroids based on two existing particle-linkage models. The proposed simplified model is a non-axisymmetric triple-particle-linkage model which consists of three particles and two massless rigid rods. With the assumption that both the total mass and the angular velocity of the simplified model are equivalent to those of the target asteroid, the number of unknown parameters for this model reduces to five. The determination of these unknown parameters is achieved through connecting the simplified model with the polyhedral model by matching the positions of their equilibrium points. A method based on nonlinear optimization is proposed to minimize the total matching error of all external equilibrium points. The proposed simplified model is applied for the realistic asteroids 243 Ida, 433 Eros and 1996 HW1. The results indicate that the non-axisymmetric triple-particle-linkage model has advantages over the two existing particle-linkage models in terms of matching accuracy. Moreover, it is verified that the topological cases of the equilibrium points are not changed by use of the proposed simplified model.

**Acknowledgements** The work described in this paper was supported by the National Natural Science Foundation of China (Grant No. 11672126), the Innovation Funded Project of Shanghai Aerospace Science and Technology (Grant Nos. SAST2017032 and SAST2015036) and the Scientific Research Foundation for New Staffs of Nanjing University of Aeronautics and Astronautics (Grant No. 1011-YAH17071). The authors fully appreciate their financial supports.

## References

Bartczak, P., & Breiter, S. 2003, Celestial Mechanics and Dynamical Astronomy, 86, 131
Bartczak, P., Breiter, S., & Jusiel, P. 2006, Celestial Mechanics and Dynamical Astronomy, 96, 31
Chanut, T. G. G., Aljbaae, S., & Carruba, V. 2015, MNRAS, 450, 3742
Chermnykh, S. V. 1987, Leningradskii Universitet Vestnik Matematika Mekhanika Astronomiia, 73
Elipe, A., & Lara, M. 2003, J. Astronaut. Sci., 51, 391
Goździewski, K. 1998, Celestial Mechanics and Dynamical Astronomy, 70, 41
Jiang, Y. 2015, Earth Moon and Planets, 115, 31
Jiang, Y., Baoyin, H., Li, J., & Li, H. 2014, Ap&SS, 349, 83
Lan, L., Yang, H., Baoyin, H., & Li, J. 2017, Ap&SS, 362, 169
Li, X., Gao, A., & Qiao, D. 2017, Ap&SS, 362, 85
Li, X., Qiao, D., & Cui, P. 2013, Ap&SS, 348, 417
Liu, X., Baoyin, H., & Ma, X. 2011, Ap&SS, 333, 409
Magri, C., Howell, E., Nolan, M. C., et al. 2017, NASA Planetary Data System (*https://sbn.psi.edu/pds/resource/shape8567.html*)
Prieto-Llanos, T., & Gomez-Tierno, M. A. 1994, Journal of Guidance Control Dynamics, 17, 787
Riaguas, A., Elipe, A., & López-Moratalla, T. 2001, Celestial Mechanics and Dynamical Astronomy, 81, 235
Scheeres, D. J., Williams, B. G., & Miller, J. K. 2000, Journal of Guidance Control Dynamics, 23, 466
Shang, H., Wu, X., & Cui, P. 2015, Ap&SS, 355, 69
Stooke, P. 2016, NASA Planetary Data System (*http://adsabs.harvard.edu/abs/2016PDSS..240.....S*)
Thomas, P., Joseph, J., Carcich, B., & Raugh, A. C., 2001, NASA Planetary Data System (*https://sbn.psi.edu/pds/resource/nearmod.html*)
Wang, W., Yang, H., Zhang, W., & Ma, G. 2017, Ap&SS, 362, 229
Wang, X., Jiang, Y., & Gong, S. 2014, Ap&SS, 353, 105
Werner, R. A., & Scheeres, D. J. 1996, Celestial Mechanics and Dynamical Astronomy, 65, 313
Yang, H., Bai, X., & Li, S. 2018, Journal of Guidance, Control, and Dynamics, 41, 6, 1308
Yang, H., Baoyin, H., Bai, X., & Li, J. 2017, Ap&SS, 362, 27
Yang, H.-W., Zeng, X.-Y., & Baoyin, H. 2015, RAA (Research in Astronomy and Astrophysics), 15, 1571
Yu, Y., & Baoyin, H. 2012a, MNRAS, 427, 872
Yu, Y., & Baoyin, H. 2012b, AJ, 143, 62
Yu, Y., Baoyin, H., & Jiang, Y. 2015, MNRAS, 453, 3269
Zeng, X., Jiang, F., Li, J., & Baoyin, H. 2015, Ap&SS, 356, 29
Zeng, X.-Y., Liu, X.-D., & Li, J.-F. 2017, RAA (Research in Astronomy and Astrophysics), 17, 2
Zeng, X., Zhang, Y., Yu, Y., & Liu, X. 2018, AJ, 155, 85